Delft University of Technology

Delft Center for Systems and Control

Technical report 20-005

A robust MPC energy scheduling strategy for multi-carrier microgrids*

R. Carli, G. Cavone, T. Pippia, B. De Schutter, and M. Dotoli

If you want to cite this report, please use the following reference instead:
R. Carli, G. Cavone, T. Pippia, B. De Schutter, and M. Dotoli, "A robust MPC energy scheduling strategy for multi-carrier microgrids," *Proceedings of the 16th IEEE International Conference on Automation Science and Engineering (CASE 2020)*, Virtual Conference, pp. 152–158, Aug. 2020. doi:10.1109/CASE48305.2020.9216875

Delft Center for Systems and Control
Delft University of Technology
Mekelweg 2, 2628 CD Delft
The Netherlands
phone: +31-15-278.24.73 (secretary)
URL: `https://www.dcsc.tudelft.nl`

*This report can also be downloaded via `https://pub.deschutter.info/abs/20_005.html`

A Robust MPC Energy Scheduling Strategy for Multi-Carrier Microgrids

Raffaele Carli[1], *Member, IEEE,* Graziana Cavone[1], *Member, IEEE,* Tomas Pippia[2], Bart De Schutter[2], *Fellow, IEEE,* and Mariagrazia Dotoli[1], *Senior Member, IEEE*

***Abstract*— We present a Robust Model Predictive Control (RMPC) approach for multi-carrier microgrids, i.e., microgrids based on gas and electricity. The microgrid that we consider includes thermal loads, electrical loads, renewable energy sources, energy storage systems, heat pumps, and combined heat and power plants. Moreover, the system under control is affected by several external disturbances, e.g., uncertainty in renewable energy generation, electrical and thermal demand. The goal of the controller is to minimize the overall economical cost and the energy exchange with the main grid, while guaranteeing comfort. Whereas several RMPC methods have been developed for electrical or thermal microgrids, little or no attention has been devoted to robust control of multi-carrier microgrids. Therefore, we consider a novel RMPC algorithm that can improve the performance with respect to classical deterministic Model Predictive Control (Det-MPC) controllers in the context of multi-carrier microgrids. The RMPC method relies on the box-uncertainty-set robust optimization, where uncertain parameters are assumed to take their values from different intervals independently. The RMPC approach is able to successfully satisfy the constraints even in the presence of the mentioned disturbances. Simulations of a realistic residential case study show the benefits of the proposed approach with respect to Det-MPC controllers.**

***Index Terms*— Optimization and Optimal Control; Energy and Environment-Aware Automation; Microgrid; Set-based Uncertainty; Robust Model Predictive Control.**

I. Introduction

The ongoing energy transition has led to many changes in the energy networks in the recent years [1]. Both electrical and thermal networks have benefited from the technological advancements and from an increased share of renewables. Moreover, technological improvements have made it possible to consider grids of small size, i.e., microgrids [2], that have many benefits, e.g., decrease in the energy waste due to reduced transportation. Microgrids also provide high resilience and reliability and they can be electrical, thermal, or mixed. However, due to the uncertainty in the renewable energy generation and loads, microgrids open many challenges that still have to be fully faced.

[1] R. Carli, G. Cavone, and M. Dotoli are with the Dept. of Electrical and Information Engineering, Polytechnic of Bari, Bari, Italy (email: {raffaele.carli, graziana.cavone, mariagrazia.dotoli}@poliba.it).

[2] T. Pippia and B. De Schutter are with the Delft Center for Systems and Control, Delft University of Technology, Delft, The Netherlands (email: {t.m.pippia, b.deschutter}@tudelft.nl).

This work received funding from the European Union's Horizon 2020 research and innovation programme under the Marie Skłodowska–Curie grant agreement No. 675318 (INCITE), from the Italian University and Research Ministry under project RAFAEL (National Research Program, contract No. ARS01_00305), and from the National Natural Science Foundation of China under Grant No. 61950410604.

Indeed, in microgrid control algorithms, the usual objective is to minimize an economical goal while simultaneously achieving other goals, e.g., minimizing the exchange of energy with the main grid [3]. In the literature context of microgrid control, Model Predictive Control (MPC) [4] stands out as one of the main control tools. MPC is an optimization-based control approach, allowing to include constraints and objectives in the control problem formulation. Moreover, given the presence of several unknown disturbances, it is important to consider an MPC controller that can properly handle the system uncertainties, because a deterministic MPC (Det-MPC) approach might lead to poor performance. In this regard, two main classes of MPC have been proposed to deal with disturbances, i.e., stochastic MPC and robust MPC (RMPC) [5]. The adoption of either method depends on the considered application. However, a stochastic controller relies on a large amount of prior data, which might not be available in the context of microgrid control. On the other hand, a robust controller can properly handle every possible disturbance, as long as it stays within predefined bounds, guaranteeing constraint satisfaction at all times, by having information only on the upper and lower bounds of the disturbances, which are easy to obtain. Moreover, RMPC is useful in applications in which a safe operation of the grid as well as hard constraints on the amount of power exchanged with the main grid have to be guaranteed [6].

Several MPC control schemes for microgrids have recently been studied [6]–[14]. In [7], a modeling framework for electrical microgrid energy management systems is presented. Similarly, paper [8] presents a thermal microgrid modeling framework and a Det-MPC approach, considering district heating, thermal energy storage, and flexible loads. MPC algorithms for multi-carrier microgrids have been proposed in [6], [9], [10]. In particular, [9] presents a stochastic MPC approach for microgrids containing both thermal and electrical units, by using a two-stage optimization strategy. The manuscript [10] presents an MPC approach for the energy management of a microgrid comprising both electrical and thermal units, providing also stability of the controlled system, where, however, the controller is deterministic.

For what concerns RMPC, some works have considered its application to microgrids [6], [11]–[14]. In [11], a min-max RMPC algorithm for fuel cell cars in a microgrid is presented. Vehicles are used as a power plant when they are parked and not in use. In [12], authors present an economic RMPC controller subject to constraints on the operation limits of the microgrid components and on the

energy balances under variations of the expected loads, using a constraint tightening strategy. The authors of [13] present an RMPC method that considers three types of uncertainty scenarios and uncertainty budgets for islanded microgrids. Paper [14] presents an RMPC controller in which the degree of uncertainty of the method proposed in [15] is used for islanded electrical microgrids. By using this method, the controller can be made more or less conservative, based on the importance given to the constraint satisfaction. Paper [6] presents an RMPC approach for multi-carrier microgrids, focusing on a demand response program of the United Kingdom national grid; such a program provides security of supply to the main grid while the flexibility provider is economically rewarded for its commitment. Note that, while all these papers, i.e., [6], [11]–[14], present an RMPC controller, they consider a fully electrical microgrid without any thermal equipment, with the only exception of [6]. While [6] does consider a multi-carrier microgrid, its focus is limited to the short-term operating reserve in the United Kingdom context.

From the previous discussion and to best of the authors' knowledge, little attention has been devoted in the related literature to RMPC algorithms for microgrids that contain *both* electricity and heating systems. Indeed, articles from the literature that present RMPC algorithms deal mostly with electrical microgrids without considering heating systems. On the other hand, the few papers that do consider both systems do not tackle the challenge of uncertainties acting in the microgrid, i.e., they do not adopt an RMPC approach. Therefore, in this work, we address the robust optimal control of a multi-carrier microgrid equipped with several elements, including thermal loads (TLs), non-controllable electrical loads or infeasible (NCELs) and controllable or feasible electrical loads (CELs), renewable energy sources (RESs), electrical energy storage systems (EESSs), thermal energy storage systems (TESSs), heat pumps (HPs), combined heat and power (CHPs) units, and auxiliary boiler. Differently from the related literature, we propose a novel tractable RMPC algorithm that can improve the performance with respect to Det-MPC controllers. In particular, the proposed RMPC method relies on the box-uncertainty-set robust optimization [16], where uncertain parameters are assumed to take their values from different intervals independently. The presented approach is able to successfully satisfy the constraints even in the presence of disturbances in renewable energy generation, and in the electrical and thermal demand.

II. System Model

In this section we describe the system under control extending the model presented by some of the authors in [3]. We suppose that the prediction window at time t, $\mathcal{H}(t) = \{t+1, \dots, t+H\}$, has a fixed length H of equally spaced time intervals, which moves ahead at every time slot t. The proposed scheme is illustrated in Fig. 1. We consider a typical multi-carrier microgrid, where the electrical and thermal demands are supplied using the connection to the electricity and natural gas main grids and the interaction

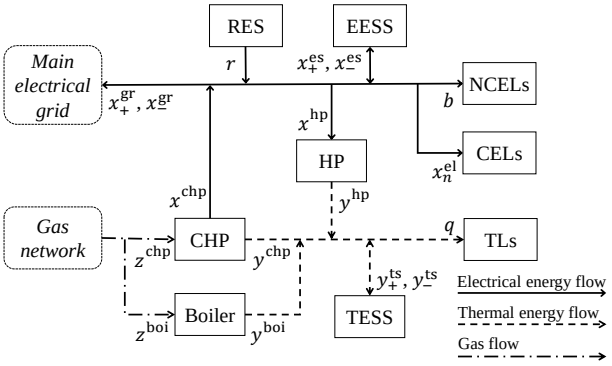

Fig. 1. Scheme of energy flows and connections.

with the internal facilities such as the RES, HP, CHP unit, auxiliary boiler, EESS, and TESS. We assume that the exchange of electricity between the microgrid and the electrical main grid is bidirectional (i.e., both selling and buying are allowed), while the exchange with the gas main grid is unidirectional (i.e., only buying is allowed for the microgrid).

A. Electrical and Thermal Loads

As for the electrical loads, we assume that the microgrid is equipped with NCELs, whose operation time cannot be shifted in time and whose electrical consumption profile cannot be modulated. We introduce a column vector of H input parameters $\mathbf{b}(t) := [b\,(t+1), \dots, b\,(t+H)]^{\top}$ to denote the overall energy consumption profile of the NCELs at time t.

Secondly, we assume that the grid is also equipped with CELs, which are loads with flexible and programmable operation. We introduce a column vector $\mathbf{x}^{\mathrm{el}}_n(t) := [x^{\mathrm{el}}_n\,(t+1), \dots, x^{\mathrm{el}}_n\,(t+H)]^{\top}$ with H decision variables referring to the energy consumption profile of each CEL $n \in \mathcal{N}^{\mathrm{cel}} = \{1, ..., N^{\mathrm{cel}}\}$. We collect the profiles of all the N^{cel} CELs in a column vector $\mathbf{x}^{\mathrm{el}}(t) := [\mathbf{x}^{\mathrm{el}}_1(t)^{\top}, \dots, \mathbf{x}^{\mathrm{el}}_N(t)^{\top}]^{\top}$ with length NH. Due to operational requirements, CELs are restricted by minimum and maximum operating levels. We use two column vectors of H input parameters $\bar{\mathbf{l}}_n(t) := [\bar{l}_n\,(t+1), \dots, \bar{l}_n\,(t+H)]^{\top}$ and $\underline{\mathbf{l}}_n(t) := [\underline{l}_n\,(t+1), \dots, \underline{l}_n\,(t+H)]^{\top}$ to indicate the maximum and minimum energy level for each CEL n, respectively. Furthermore, for each CEL n a certain amount of energy $L_n(t)$ has to be consumed in the given time window. Summing up, the following constraints hold:

$$\underline{\mathbf{l}}_n(t) \leq \mathbf{x}^{\mathrm{el}}_n(t) \leq \bar{\mathbf{l}}_n(t), n \in \mathcal{N}^{\mathrm{cel}} \quad (1)$$

$$\mathbf{1}_H{}^{\top}\mathbf{x}^{\mathrm{el}}_n(t) = L_n(t), n \in \mathcal{N}^{\mathrm{cel}} \quad (2)$$

where $\mathbf{1}_H$ denotes an H-dimensional vector with all ones.

As for the thermal loads, we denote the thermal load consumption profile over the time horizon by a vector of H input parameters $\mathbf{q}(t) := [q\,(t+1), \dots, q\,(t+H)]^{\top}$ accounting for both the space heating and water demand.

B. Renewable Energy Source

We assume that the microgrid incorporates a RES, e.g., a photo-voltaic (PV) panel or domestic wind turbine. We

define a column vector of H input parameters $\mathbf{r}(t) := [r(t+1), \ldots, r(t+H)]^\top$ collecting the energy profile produced by the RES.

C. Heat Pump

The main indicator for measuring the HP performance is the so-called Coefficient of Performance (COP), which is generally a function of the temperature level of the indoor environment and temperature difference between indoor and outdoor temperature. In this work the COP - denoted as η^{hp} - is assumed to be constant over the time horizon. The corresponding power and heat flow is thus described by:

$$\mathbf{y}^{\mathrm{hp}}(t) = \eta^{\mathrm{hp}}\, \mathbf{x}^{\mathrm{hp}}(t) \tag{3}$$

where $\mathbf{x}^{\mathrm{hp}}(t) := [x^{\mathrm{xp}}(t+1), \ldots, x^{\mathrm{hp}}(t+H)]^\top$ and $\mathbf{y}^{\mathrm{hp}}(t) := [y^{\mathrm{hp}}(t+1), \ldots, y^{\mathrm{hp}}(t+H)]^\top$ are the required input electrical energy and the output thermal energy produced by the HP over the time horizon, respectively. Due to operational requirements, the thermal energy produced by the HP is restricted by the minimum and maximum operating levels $\underline{p}^{\mathrm{hp}}$ and $\overline{p}^{\mathrm{hp}}$:

$$\underline{p}^{\mathrm{hp}} \mathbf{1}_H \leq \mathbf{y}^{\mathrm{hp}}(t) \leq \overline{p}^{\mathrm{hp}} \mathbf{1}_H. \tag{4}$$

D. Gas Boiler

We assume that the microgrid includes a gas-fired boiler. Such a boiler is characterized by high efficiency in the burning process (i.e., its efficiency ratio η^{boi} is around 100%) and fast dynamics (i.e., they are able to react to sudden changes in hot water demand) . This energy conversion process can be modeled as follows:

$$\mathbf{y}^{\mathrm{boi}}(t) = \eta^{\mathrm{boi}} \mathbf{z}^{\mathrm{boi}}(t) \tag{5}$$

where $\mathbf{y}^{\mathrm{boi}}(t) := [y^{\mathrm{boi}}(t+1), \ldots, y^{\mathrm{boi}}(t+H)]^\top$ and $\mathbf{z}^{\mathrm{boi}}(t) := [z^{\mathrm{boi}}(t+1), \ldots, z^{\mathrm{boi}}(t+H)]^\top$ represent the generated heating and the amount of gas burned by the auxiliary boiler over the time horizon, respectively. Due to operational requirements, the thermal energy produced by the boiler is restricted by the minimum and maximum operating levels $\underline{p}^{\mathrm{boi}}$ and $\overline{p}^{\mathrm{boi}}$:

$$\underline{p}^{\mathrm{boi}} \mathbf{1}_H \leq \mathbf{y}^{\mathrm{boi}}(t) \leq \overline{p}^{\mathrm{boi}} \mathbf{1}_H. \tag{6}$$

E. Combined Heat and Power Unit

CHP or cogeneration units are generators that simultaneously produce heat and electrical (or mechanical) energy from a single fuel source (usually natural gas). Electricity production and heat generation in the CHP system are strongly correlated at any time instant, as indicated by:

$$\mathbf{x}^{\mathrm{chp}}(t) = \eta_{\mathrm{e}}^{\mathrm{chp}} \mathbf{z}^{\mathrm{chp}}(t) \tag{7}$$

$$\mathbf{y}^{\mathrm{chp}}(t) = \eta_{\mathrm{t}}^{\mathrm{chp}} \mathbf{z}^{\mathrm{chp}}(t) \tag{8}$$

where $\eta_{\mathrm{e}}^{\mathrm{chp}}$ and $\eta_{\mathrm{t}}^{\mathrm{chp}}$ are respectively the thermal and electrical efficiency of the CHP, whilst $\mathbf{z}^{\mathrm{chp}}(t) = [z^{\mathrm{chp}}(t+1), \ldots, z^{\mathrm{chp}}(t+H)]^\top$ represents the instantaneous amount of gas burned by the CHP over the time horizon. Due to operational requirements, the electrical and thermal energy produced by the CHP unit is restricted by the minimum and maximum electrical and thermal operating levels $\underline{l}^{\mathrm{chp}}$, $\overline{l}^{\mathrm{chp}}$, $\underline{p}^{\mathrm{chp}}$, and $\overline{p}^{\mathrm{chp}}$:

$$\underline{l}^{\mathrm{chp}} \mathbf{1}_H \leq \mathbf{x}^{\mathrm{chp}}(t) \leq \overline{l}^{\mathrm{chp}} \mathbf{1}_H \tag{9}$$

$$\underline{p}^{\mathrm{chp}} \mathbf{1}_H \leq \mathbf{y}^{\mathrm{chp}}(t) \leq \overline{p}^{\mathrm{chp}} \mathbf{1}_H. \tag{10}$$

F. Electrical and Thermal Energy Storage System

We model the EESS as a first-order discrete-time buffer, independently from the actual storage technology. To define the charging/discharging activities of the EESS within the time horizon, we introduce two vectors $\mathbf{x}_+^{\mathrm{es}}(t) := \left[x_+^{\mathrm{es}}(t+1), \ldots, x_+^{\mathrm{es}}(t+H)\right]^\top$ and $\mathbf{x}_-^{\mathrm{es}}(t) := \left[x_-^{\mathrm{es}}(t+1), \ldots, x_-^{\mathrm{es}}(t+H)\right]^\top$, each collecting H decision variables, where $x_+^{\mathrm{es}}(t+h)$ and $x_-^{\mathrm{es}}(t+h)$ is the energy stored in and released by the EESS at time slot $t+h$, respectively. The charge level is computed by:

$$s^{\mathrm{es}}(t+h) = s^{\mathrm{es}}(t+h-1) + \eta_+^{\mathrm{es}} x_+^{\mathrm{es}}(t+h) - \frac{1}{\eta_-^{\mathrm{es}}} x_-^{\mathrm{es}}(t+h), \quad h \in \mathcal{H}(t) \tag{11}$$

where η_+^{es} and η_-^{es} are the charging and discharging efficiencies, respectively. The maximum charge level is bounded by the minimum and maximum EESS capacity $\underline{S}^{\mathrm{es}}$ and $\overline{S}^{\mathrm{es}}$:

$$\underline{S}^{\mathrm{es}} - s^{\mathrm{es}}(t+h-1) \leq \eta_+^{\mathrm{es}} x_+^{\mathrm{es}}(t+h) - \frac{1}{\eta_-^{\mathrm{es}}} x_-^{\mathrm{es}}(t+h) \leq \overline{S}^{\mathrm{es}} - s^{\mathrm{es}}(t+h-1), \; h \in \mathcal{H}(t). \tag{12}$$

Denoting by $\overline{s}^{\mathrm{es}}$ and $\underline{s}^{\mathrm{es}}$ as the maximum charging and discharging rates, the following constraints must be satisfied:

$$0 \leq x_+^{\mathrm{es}}(t+h) \leq \delta_+^{\mathrm{es}}(t+h) \overline{s}^{\mathrm{es}}, \; h \in \mathcal{H}(t) \tag{13}$$

$$0 \leq x_-^{\mathrm{es}}(t+h) \leq \delta_-^{\mathrm{es}}(t+h) \underline{s}^{\mathrm{es}}, \; h \in \mathcal{H}(t) \tag{14}$$

where $\boldsymbol{\delta}_+^{\mathrm{es}}(t) := [\delta_+^{\mathrm{es}}(t+1), \ldots, \delta_+^{\mathrm{es}}(t+H)]^\top$ and $\boldsymbol{\delta}_-^{\mathrm{es}}(t) := [\delta_-^{\mathrm{es}}(t+1), \ldots, \delta_-^{\mathrm{es}}(t+H)]^\top$ are two vectors of supporting binary variables, introduced to avoid simultaneous charging and discharging:

$$\delta_+^{\mathrm{es}}(t+h) \in \{0,1\}, \delta_-^{\mathrm{es}}(t+h) \in \{0,1\}, h \in \mathcal{H}(t) \tag{15}$$

$$\delta_+^{\mathrm{es}}(t+h) + \delta_-^{\mathrm{es}}(t+h) \leq 1, h \in \mathcal{H}(t). \tag{16}$$

Note that it holds $\delta_+^{\mathrm{es}}(t+h) = 1$ or $\delta_+^{\mathrm{es}}(t+h) = 0$ if the EESS is charged or is not charged at time slot $t+h$, respectively; similarly, it holds $\delta_-^{\mathrm{es}}(t+h) = 1$ or $\delta_-^{\mathrm{es}}(t+h) = 0$ if the EESS is discharged or is not discharged at time slot $t+h$, respectively.

As for the TESS, we model this device similarly to the EESS. We define two vectors $\mathbf{y}_+^{\mathrm{ts}}(t) := \left[y_+^{\mathrm{ts}}(t+1), \ldots, y_+^{\mathrm{ts}}(t+H)\right]^\top$ and $\mathbf{y}_-^{\mathrm{ts}}(t) := \left[y_-^{\mathrm{ts}}(t+1), \ldots, y_-^{\mathrm{ts}}(t+H)\right]^\top$, each collecting H decision variables, where $y_+^{\mathrm{ts}}(t+h)$ and $y_-^{\mathrm{ts}}(t+h)$ are the energy stored in and released from the TESS at any time slot $t+h$, respectively. Denoting the TESS charge level at time slot $t+h$ as $s^{\mathrm{ts}}(t+h)$, the following constraints must be satisfied:

$$s^{\mathrm{ts}}(t+h) = s^{\mathrm{ts}}(t+h-1) + \eta_+^{\mathrm{ts}} y_+^{\mathrm{ts}}(t+h) - (1/\eta^{\mathrm{ts}}) y_-^{\mathrm{ts}}(t+h), \quad h \in \mathcal{H}(t) \tag{17}$$

$$\underline{S}^{\mathrm{ts}} - s^{\mathrm{ts}}(t+h-1) \leq \eta_{+}^{\mathrm{ts}} y_{+}^{\mathrm{ts}}(t+h) - (1/\eta_{-}^{\mathrm{ts}}) y_{-}^{\mathrm{ts}}(t+h) \leq \overline{S}^{\mathrm{ts}} - s^{\mathrm{ts}}(t+h-1),\ h \in \mathcal{H}(t) \quad (18)$$

$$0 \leq y_{+}^{\mathrm{ts}}(t+h) \leq \delta_{+}^{\mathrm{ts}}(t+h)\overline{s}^{\mathrm{ts}},\ h \in \mathcal{H}(t) \quad (19)$$

$$0 \leq y_{-}^{\mathrm{ts}}(t+h) \leq \delta_{-}^{\mathrm{ts}}(t+h)\underline{s}^{\mathrm{ts}},\ h \in \mathcal{H}(t) \quad (20)$$

$$\delta_{+}^{\mathrm{ts}}(t+h) \in \{0,1\}, \delta_{-}^{\mathrm{ts}}(t+h) \in \{0,1\}, h \in \mathcal{H}(t) \quad (21)$$

$$\delta_{+}^{\mathrm{ts}}(t+h) + \delta_{-}^{\mathrm{ts}}(t+h) \leq 1, h \in \mathcal{H}(t) \quad (22)$$

where η_{+}^{ts} and η_{-}^{ts} are the charging and discharging efficiencies, $\underline{S}^{\mathrm{ts}}$ and $\overline{S}^{\mathrm{ts}}$ are the minimum and maximum capacities, $\overline{s}^{\mathrm{ts}}$ and $\underline{s}^{\mathrm{ts}}$ are the maximum charging and discharging rates, and $\boldsymbol{\delta}_{+}^{\mathrm{ts}}(t) := [\delta_{+}^{\mathrm{ts}}(t+1), \ldots, \delta_{+}^{\mathrm{ts}}(t+H)]^{\top}$ and $\boldsymbol{\delta}_{-}^{\mathrm{ts}}(t) := [\delta_{-}^{\mathrm{ts}}(t+1), \ldots, \delta_{-}^{\mathrm{ts}}(t+H)]^{\top}$ are two vectors of supporting variables with an analogous meaning as in the EESS case.

G. Electrical and Thermal Energy Flow Balance

In a multi-carrier scenario, both the electrical and thermal energy have to be balanced in the microgrid at any time instant:

$$\mathbf{x}_{+}^{\mathrm{gr}}(t) + \mathbf{r}(t) + \mathbf{x}^{\mathrm{chp}}(t) + \mathbf{x}_{-}^{\mathrm{es}}(t) = \mathbf{x}_{-}^{\mathrm{gr}}(t) + \sum_{n=1}^{N} \mathbf{x}_{n}^{\mathrm{el}}(t) + \mathbf{b}(t) + \mathbf{x}_{+}^{\mathrm{es}}(t) \quad (23)$$

$$\mathbf{q}(t) + \mathbf{y}_{+}^{\mathrm{ts}}(t) = \mathbf{y}^{\mathrm{boi}}(t) + \mathbf{y}^{\mathrm{chp}}(t) + \mathbf{y}^{\mathrm{hp}}(t) + \mathbf{y}_{-}^{\mathrm{ts}}(t) \quad (24)$$

where $\mathbf{x}_{+}^{\mathrm{gr}}(t) := \left[x_{+}^{\mathrm{gr}}(t+1), \ldots, x_{+}^{\mathrm{gr}}(t+H)\right]^{\top}$ and $\mathbf{x}_{-}^{\mathrm{gr}}(t) := \left[x_{-}^{\mathrm{gr}}(t+1), \ldots, x_{-}^{\mathrm{gr}}(t+H)\right]^{\top}$ are two column vectors with H decision variables denoting the profile of the electricity bought and sold over the time horizon, respectively.

H. Grid Pricing and Constraints

A contractual obligation is enforced by the energy provider as an additional constraint, restricting the residual microgrid energy that could be bought from and sold to the power grid to a maximum level at each time slot. We denote the maximum purchasable and salable energy profile imposed by the energy provider over the time horizon as column vectors $\overline{\mathbf{g}}(t) := [\overline{g}(t+1), \ldots, \overline{g}(t+H)]^{\top}$ and $\underline{\mathbf{g}}(t) := [\underline{g}(t+1), \ldots, \underline{g}(t+H)]^{\top}$, respectively. Thus, the values of the bought and sold energy profile over the time horizon must be subject to the following constraints:

$$\mathbf{0}_H \leq \mathbf{x}_{+}^{\mathrm{gr}}(t) \leq \overline{\mathbf{g}}(t) \circ \boldsymbol{\delta}_{+}^{\mathrm{gr}}(t) \quad (25)$$

$$\mathbf{0}_H \leq \mathbf{x}_{-}^{\mathrm{gr}}(t) \leq \underline{\mathbf{g}}(t) \circ \boldsymbol{\delta}_{-}^{\mathrm{gr}}(t) \quad (26)$$

where symbol $\circ$ indicates the entrywise product and $\boldsymbol{\delta}_{+}^{\mathrm{gr}}(t) := [\delta_{+}^{\mathrm{gr}}(t+1), \ldots, \delta_{+}^{\mathrm{gr}}(t+H)]^{\top}$ and $\boldsymbol{\delta}_{-}^{\mathrm{gr}}(t) := [\delta_{-}^{\mathrm{gr}}(t+1), \ldots, \delta_{-}^{\mathrm{gr}}(t+H)]^{\top}$ are two vectors of supporting binary variables introduced to avoid that energy is simultaneously bought from and sold to the power grid:

$$\boldsymbol{\delta}_{+}^{\mathrm{gr}}(t) \in \{0,1\}^{H}, \boldsymbol{\delta}_{-}^{\mathrm{gr}}(t) \in \{0,1\}^{H} \quad (27)$$

$$\boldsymbol{\delta}_{+}^{\mathrm{gr}}(t) + \boldsymbol{\delta}_{-}^{\mathrm{gr}}(t) \leq \mathbf{1}_H. \quad (28)$$

Note that it holds $\delta_{+}^{\mathrm{gr}}(t+h) = 1$ or $\delta_{+}^{\mathrm{gr}}(t+h) = 0$ if the microgrid buys or does not buy energy from the main grid at time slot $t+h$, respectively; similarly, it holds $\delta_{-}^{\mathrm{gr}}(t+h) = 1$ or $\delta_{-}^{\mathrm{gr}}(t+h) = 0$ if the microgrid sells or does not sell energy to the main grid at time slot $t+h$, respectively. We assume that the pricing function for the electricity bought from and sold to the main grid is linear. In particular, we consider two different sets of pricing coefficients $\boldsymbol{\kappa}_{+}(t) := [\kappa_{+}(t+1), \ldots, \kappa_{+}(t+H)]^{\top}$ and $\boldsymbol{\kappa}_{-}(t) := [\kappa_{-}(t+1), \ldots, \kappa_{-}(t+H)]^{\top}$ for the electricity bought from and sold to the grid, respectively. The electricity cost incurred by the microgrid over the time horizon is defined as follows: $c^{\mathrm{gr}} = \boldsymbol{\kappa}_{+}(t)^{\top}\mathbf{x}_{+}^{\mathrm{gr}}(t) - \boldsymbol{\kappa}_{-}(t)^{\top}\mathbf{x}_{-}^{\mathrm{gr}}(t)$.

In order to encourage self-consumption in the microgrid, we introduce a penalty cost that limits the amount of energy exchanged per time slot by the microgrid with the main grid in a given range $[-\underline{\mathbf{g}}^{\pi}, \overline{\mathbf{g}}^{\pi}]$. To this aim, we introduce two vectors of H slack variables $\boldsymbol{\psi}_{+}(t) := [\psi_{+}(t+1), \ldots, \psi_{+}(t+H)]^{\top}$ and $\boldsymbol{\psi}_{-}(t) := [\psi_{-}(t+1), \ldots, \psi_{-}(t+H)]^{\top}$ denoting the profile of the surplus of energy bought from and sold to the main grid with respect to the bounding $\underline{\mathbf{g}}^{\pi}$ and $\overline{\mathbf{g}}^{\pi}$, respectively:

$$\boldsymbol{\psi}_{+}(t) \geq \mathbf{0}_H \quad (29)$$

$$\boldsymbol{\psi}_{+}(t) \geq \mathbf{x}_{+}^{\mathrm{gr}}(t) - \overline{\mathbf{g}}^{\pi}\mathbf{1}_H \quad (30)$$

$$\boldsymbol{\psi}_{-}(t) \geq \mathbf{0}_H \quad (31)$$

$$\boldsymbol{\psi}_{-}(t) \geq \mathbf{x}_{-}^{\mathrm{gr}}(t) - \underline{\mathbf{g}}^{\pi}\mathbf{1}_H. \quad (32)$$

Hence, the penalty cost incurred by the microgrid over the time horizon is defined with a quadratic formulation: $c^{\mathrm{pen}} = \pi\left(\boldsymbol{\psi}_{+}(t)^{\top}\boldsymbol{\psi}_{+}(t) + \boldsymbol{\psi}_{-}(t)^{\top}\boldsymbol{\psi}_{-}(t)\right)$, where π indicates a weighting factor.

Finally, we assume that the pricing function for the natural gas bought from the main grid is linear. Introducing the vector of gas pricing coefficients $\boldsymbol{\nu}(t) := [\nu(t+1), \ldots, \nu(t+H)]^{\top}$, the gas cost incurred by the microgrid over the time horizon is defined as follows: $c^{\mathrm{gas}} = \boldsymbol{\nu}(t)^{\top}\left(\mathbf{z}^{\mathrm{boi}}(t) + \mathbf{z}^{\mathrm{chp}}(t)\right)$.

III. Deterministic Energy Scheduling Strategy

In the preliminary deterministic MPC approach to the energy scheduling, uncertainty is disregarded and the scheduling problem is solved based on nominal forecasted values of electrical and thermal energy demand and RES generation. We first formulate the problem aiming at determining the optimal microgrid energy schedule including the operations of controllable CELs and HP, the amount of electricity to be bought from and sold to the grid, the amount of natural gas to be bought for the boiler and CHP unit operations, and the charging/discharging strategy for the EESS and TESS over the time window $\mathcal{H}(t)$:

$$\min\left(c^{\mathrm{gr}} + c^{\mathrm{pen}} + c^{\mathrm{gas}}\right) \quad \text{s.t. (1)-(32).} \quad (33)$$

where $\mathbf{x}_{+}^{\mathrm{gr}}(t)$, $\mathbf{x}_{-}^{\mathrm{gr}}(t)$, $\mathbf{x}^{\mathrm{el}}(t)$, $\mathbf{x}^{\mathrm{hp}}(t)$, $\mathbf{x}^{\mathrm{chp}}(t)$, $\mathbf{x}_{+}^{\mathrm{es}}(t)$, $\mathbf{x}_{-}^{\mathrm{es}}(t)$, $\mathbf{y}^{\mathrm{chp}}(t)$, $\mathbf{y}^{\mathrm{boi}}(t)$, $\mathbf{y}_{+}^{\mathrm{ts}}(t)$, $\mathbf{y}_{-}^{\mathrm{ts}}(t)$, $\mathbf{z}^{\mathrm{boi}}(t)$, $\mathbf{z}^{\mathrm{chp}}(t)$, $\boldsymbol{\delta}_{+}^{\mathrm{es}}(t)$, $\boldsymbol{\delta}_{-}^{\mathrm{es}}(t)$, $\boldsymbol{\delta}_{+}^{\mathrm{ts}}(t)$, $\boldsymbol{\delta}_{-}^{\mathrm{ts}}(t)$, $\boldsymbol{\delta}_{+}^{\mathrm{gr}}(t)$, $\boldsymbol{\delta}_{-}^{\mathrm{gr}}(t)$, $\boldsymbol{\psi}_{+}(t)$, $\boldsymbol{\psi}_{-}(t)$ form the set of

decision variables. The real-time optimization problem (33) - that is labeled *deterministic* or *nominal* - is iteratively solved at each time slot t in accordance with the receding horizon paradigm, based on the most recent input data. Only the results referring to the first time slot are applied to the system as the optimal control signals, whilst the horizon is shifted ahead. Then, for the next time slot, a new optimization problem is solved using the updated information on forecasts and system states. The resulting closed-loop control algorithm is referred to as *deterministic* MPC.

IV. Robust Energy Scheduling Strategy

The previously defined deterministic scheduling problem unrealistically assumes perfect knowledge of electrical and thermal energy demand and RES generation (i.e., of vectors $\mathbf{b}$, $\mathbf{q}$, and $\mathbf{r}$). However, the variation in the forecast of these profiles may cause a large deviation from the optimum in the obtained results, leading to inefficient scheduling. Following the so-called set-based uncertainty model [16], we define a computationally tractable method to tackle uncertainty, which consists in finding the solutions that are feasible for any realization of uncertainty in a given set.

A. Data Uncertainty Set Definition

Following the approach proposed in [17], we define the uncertainty set as a box. However, differently from [17], in this paper we adopt a mechanism to adjust the conservatism of solutions based on tunable scalar parameters. In particular, introducing the so-called robustness factors (also known as budgets of uncertainty) γ_b, γ_q, γ_r related to NCELs, TLs, and RES generation, respectively, the box uncertainty sets related to the time window $\mathcal{H}(t)$ are defined as follows:

$$\mathbf{b}(t) - \gamma_b \hat{\mathbf{b}}(t) \leq \widetilde{\mathbf{b}}(t) \leq \mathbf{b}(t) + \gamma_b \hat{\mathbf{b}}(t) \tag{34}$$

$$\mathbf{q}(t) - \gamma_q \hat{\mathbf{q}}(t) \leq \widetilde{\mathbf{q}}(t) \leq \mathbf{q}(t) + \gamma_q \hat{\mathbf{q}}(t) \tag{35}$$

$$\mathbf{r}(t) - \gamma_r \hat{\mathbf{r}}(t) \leq \widetilde{\mathbf{r}}(t) \leq \mathbf{r}(t) + \gamma_r \hat{\mathbf{r}}(t) \tag{36}$$

where $\mathbf{b}$, $\mathbf{q}$, and $\mathbf{r}$ and $\widetilde{\mathbf{b}}$, $\widetilde{\mathbf{q}}$, and $\widetilde{\mathbf{r}}$ are the nominal and uncertain profiles of NCELs, TLs, and RES generation, respectively, whilst $\hat{\mathbf{b}}$, $\hat{\mathbf{q}}$, and $\hat{\mathbf{r}}$ denote the semi-amplitude profiles of the uncertain variables variations. We finally assume that both nominal and semi-amplitude values are available based on historical data.

B. Robust MPC Formulation

We preliminary note that uncertainty affects the constraints of (33). Replacing $\widetilde{\mathbf{b}}(t)$, $\widetilde{\mathbf{q}}(t)$, and $\widetilde{\mathbf{r}}(t)$ defined in (34)-(36) to $\mathbf{b}(t)$, $\mathbf{q}(t)$, and $\mathbf{r}(t)$ in constraints (23)-(24), (33) turns into a robust optimization problem. Leveraging on the box-uncertainty-set in (34)-(36), we can straightforwardly provide the *robust counterpart* of the optimization problem (33), which aims at achieving a solution that is feasible for any realization of the uncertainty within the defined uncertainty set. The robust counterpart is given by the following Mixed Integer Quadratic Programming (MIQP) problem:

$$\min \left(c^{\mathrm{gr}} + c^{\mathrm{pen}} + c^{\mathrm{gas}}\right) \tag{37}$$

$$\text{s.t. (1)-(22), (25)-(32), and}$$

$$\mathbf{x}_{+}^{\mathrm{gr}}(t) + \mathbf{r}(t) - \gamma_r \hat{\mathbf{r}}(t) + \mathbf{x}^{\mathrm{chp}}(t) + \mathbf{x}_{-}^{\mathrm{es}}(t) = \mathbf{x}_{-}^{\mathrm{gr}}(t) + \sum_{n=1}^{N} \mathbf{x}_{n}^{\mathrm{el}}(t) + \mathbf{b}(t) + \gamma_b \hat{\mathbf{b}}(t) + \mathbf{x}_{+}^{\mathrm{es}}(t) \tag{38}$$

$$\mathbf{q}(t) + \gamma_q \hat{\mathbf{q}}(t) + \mathbf{y}_{+}^{\mathrm{ts}}(t) = \mathbf{y}^{\mathrm{boi}}(t) + \mathbf{y}^{\mathrm{chp}}(t) + \mathbf{y}^{\mathrm{hp}}(t) + \mathbf{y}_{-}^{\mathrm{ts}}(t). \tag{39}$$

By solving the robust problem (37)-(39), the energy schedule can be obtained with different robustness levels. Indeed, the robustness of the energy schedule varies with the robustness factors γ_b, γ_q, and γ_r. Here, the role of γ_b, γ_q, and γ_r is to adjust the robustness of the proposed scheduling method against the level of conservativeness of the solution. For $\gamma_b = \gamma_q = \gamma_r = 0$, the problem is solved without considering forecast uncertainties (i.e., deterministic scheduling). The obtained results thus refer to the most optimistic case. Instead, for $\gamma_b = \gamma_q = \gamma_r = 1$, the largest amount of uncertainty is considered. Hence, uncertainties are fully addressed during the operations, but the problem refers to the most conservative case (i.e., the worst case over all the possible realizations of the uncertain variables). To curtail the level of conservativeness in the solution, the value of these parameters can be tuned between 0 and 1: the optimization results over different values of the robustness factors can be observed to choose the best solution in terms of trade-off between cost and conservatism [16].

We finally remark that, similarly to the deterministic case, the robust problem (37)-(39) is solved iteratively at each time slot t in accordance with the receding horizon principle. The resulting closed-loop control algorithm is referred to as *robust* MPC (RMPC).

V. Numerical Experiments

A. System Setup

In this section, the effectiveness of the proposed RMPC control scheme for multi-carrier microgrids is tested on three different scenarios of a realistic residential case study. The multi-carrier microgrid is assumed to be installed in a residential building in the Netherlands, including $N = 4$ households. The system is characterized by electrical and thermal demand profiles calculated on the basis of aggregated Dutch national data [18] for year 2018. The average yearly demand of electricity and thermal energy for a household amounts respectively to 3.5 MWh and 14.0 MWh. The electrical demand is partitioned into CELs and NCELs, which are equal to 1.5 MWh and 2 MWh, respectively. In this work we compute the profile of the hourly electrical non-controllable loads $b(t)$ [kWh] as a function of the available real data [18] as follows: $b(t) = N \frac{B(t)}{\sum_{i=1}^{T} B(i)} D_{\mathrm{Y}}^{\mathrm{el}}$ with $t = 1, \ldots, T$, where: $D_{\mathrm{Y}}^{\mathrm{el}}$ [kWh] is the hourly average residential electrical demand for NCELs over one year; $B(t)$ [kWh] is the hourly residential electrical demand for NCELs; $\sum_{i=1}^{T} B(i)$ is the total residential electrical demand for NCELs; $T = 8760$ is the simulation horizon (i.e., one year, time step 1 h).

Similarly, the profile of the hourly thermal demand $q(t)$ [kWh] based on the aggregated national Dutch data [18] is: $q(t) = N \frac{Q^{\mathrm{SH}}(t) + Q^{\mathrm{HW}}(t)}{\sum_{i=1}^{T} (Q^{\mathrm{SH}}(i) + Q^{\mathrm{HW}}(i))} D_{\mathrm{Y}}^{\mathrm{tl}}$ with $t = 1, \ldots, T$, where:

TABLE I

TECHNICAL PARAMETERS OF THE SYSTEM DEVICES

Parameter	Value	Unit
$\eta_{\mathrm{e}}^{\mathrm{chp}}$	0.20	-
$\eta_{\mathrm{t}}^{\mathrm{chp}}$	0.80	-
$\underline{l}^{\mathrm{chp}}$	1	kWh
$\overline{l}^{\mathrm{chp}}$, $\overline{p}^{\mathrm{boi}}$	7	kWh
$\underline{p}^{\mathrm{chp}}$	4	kWh
$\overline{p}^{\mathrm{chp}}$	28	kWh
η^{hp}	3.5	-
$\underline{p}^{\mathrm{hp}}$	1.75	kWh
$\overline{p}^{\mathrm{hp}}$	21	kWh
η^{boi}	1	-
$\underline{p}^{\mathrm{boi}}$, $\overline{l}_2^{\mathrm{el}}$, $\overline{l}_3^{\mathrm{el}}$, $\overline{l}_4^{\mathrm{el}}$	0.5	kWh
η_+^{es},η_-^{es}	0.95	-
$\underline{s}^{\mathrm{es}}$, $\underline{s}^{\mathrm{ts}}$, $\underline{l}_2^{\mathrm{el}}$	0	kWh
$\overline{s}^{\mathrm{es}}$	5	kWh
$\underline{S}^{\mathrm{es}}$, $\underline{S}^{\mathrm{ts}}$	0	kW

Parameter	Value	Unit
$\overline{S}^{\mathrm{es}}$, $\overline{S}^{\mathrm{ts}}$	20	kW
η_+^{ts}, η_-^{ts}	0.95	-
$\overline{s}^{\mathrm{ts}}$	5	kWh
$\underline{l}_1^{\mathrm{el}}$ (12:00 - 15:59)	0.4	kWh
$\underline{l}_1^{\mathrm{el}}$ (16:00 - 11:59)	0.1	kWh
$\overline{l}_1^{\mathrm{el}}$	0.6	kWh
L_1^{el}	7.5	kW
L_2^{el}	2.5	kW
$\underline{l}_3^{\mathrm{el}}$ (12:00 - 15:59)	0.2	kWh
$\underline{l}_3^{\mathrm{el}}$ (16:00 - 11:59)	0.1	kWh
L_3^{el}	6	kW
$\underline{l}_4^{\mathrm{el}}$	0	kWh
L_4^{el}	4	kW

TABLE II

PERFORMANCE INDICES VALUES WITH VARIABLE ROBUSTNESS

	γ	0	0.25	0.5	0.75	1
Case A	EC [€]	2896	3556	4254	5047	5840
	SS	0.90	0.95	0.98	0.99	1
	FESR	0.97	0.95	0.93	0.90	0.87
	EI	0.42	0.38	0.35	0.31	0.28
Case B	EC [€]	4831	5376	5922	6525	7128
	SS	1	1	1	1	1
	FESR	0.97	0.95	0.93	0.90	0.87
	EI	0.01	0.02	0.04	0.05	0.07
Case C	EC [€]	8236	9194	10152	11125	12098
	SS	0.65	0.68	0.71	0.75	0.75
	FESR	0	0	0	0	0
	EI	0.98	0.98	0.97	0.96	0.94

TABLE III

ANALYSIS OF THE CVR (SCENARIO A) IN A MONTECARLO SIMULATION WITH 1000 RUNS

γ	0	0.25	0.5	0.75	1
CVR [%]	34.8	24.0	14.7	7.60	0.00

$D_{\mathrm{Y}}^{\mathrm{tl}}$ [kWh] is the hourly average residential thermal demand over one year; $Q^{\mathrm{SH}}(t)$ [kWh] is the hourly residential space heating thermal demand; $Q^{\mathrm{HW}}(t)$ [kWh] is the hourly residential hot water thermal demand; $\sum_{i=1}^{T}(Q^{\mathrm{SH}}(i)+Q^{\mathrm{HW}}(i))$ is the total residential thermal demand.

The considered system includes $N^{\mathrm{cel}}=4$ different CELs having constant upper and lower bounds ($\overline{l}_1^{\mathrm{el}},\overline{l}_2^{\mathrm{el}},\overline{l}_3^{\mathrm{el}},\overline{l}_4^{\mathrm{el}}$ and $\underline{l}_1^{\mathrm{el}},\underline{l}_2^{\mathrm{el}},\underline{l}_3^{\mathrm{el}},\underline{l}_4^{\mathrm{el}}$). For each controllable load, it is imposed that its cumulative power consumption cannot overcome a well-defined threshold to complete the corresponding task in the defined time horizon (i.e., 24 hours).

Furthermore, we assume that the microgrid is equipped with generation and storage technologies, as well as electrical and thermal loads, as specified in Section II. As for the storage systems, we consider a lithium-ion battery and a water storage system for water and space heating. As for the energy generation, we consider: PV panel, HP, CHP unit, and auxiliary boiler. In particular, we consider a PV panel (15 kWp capacity) the generation profile of which is calculated on the basis of the 2018 Dutch solar power time series [19]. This profile is based on the concept of Capacity Factor (CF), which is the ratio of the energy produced by a solar panel (kWh) and its maximum possible generation, i.e., the Installed Capacity (IC), $r(t)=\mathrm{CF}(t)\mathrm{IC},\ \text{with } t=1,\dots,T$. All the technical parameters that characterize the system devices and their values and units are reported in Table I.

The prices of the energy and natural gas are computed based on the prices of various Dutch retailers. In particular, we consider the price of the electricity component equal to $\kappa_+(t)=0.145$ €/kWh in the time period 9:00-21:59, while it is equal to $\kappa_+(t)=0.120$ €/kWh in the time period 22:00-8:59. The natural gas price is considered constant and equals $\nu(t)=0.08$ €/kWh [20]. The selling price, in general lower than the purchasing price (due to of taxes and transportation costs), is here reasonably assumed to be equal to $\kappa_-(t)=0.1$ €/kWh. As for the energy exchange with the main grid, we set a maximum purchase $\overline{g}(t)=8$ kWh and a maximum sale $\underline{g}(t)=8$ kWh, where the values for the soft constraints are $\overline{g}^{\pi}=12.8$ kWh and $\underline{g}^{\pi}=12.8$ kWh.

Four performance indices are considered as follows:

- the overall energy cost:

$$\mathrm{EC}=\sum_{t=1}^{T}\left(\kappa_+(t)x_+^{\mathrm{gr}}(t)-\kappa_-(t)x_-^{\mathrm{gr}}(t)+\nu(t)(z^{\mathrm{boi}}(t)+z^{\mathrm{chp}}(t))\right)$$

- the self-supply:

$$\mathrm{SS}=1-\frac{\sum_{t=1}^{T}x_-^{\mathrm{gr}}(t)}{\sum_{t=1}^{T}r(t)+x^{\mathrm{chp}}(t)}$$

- the fuel energy saving ratio:

$$\mathrm{FESR}=1-\frac{\sum_{t=1}^{T}x^{\mathrm{boi}}(t)+x^{\mathrm{chp}}(t)}{\sum_{t=1}^{T}q(t)}$$

- the energy independence:

$$\mathrm{EI}=1-\frac{\sum_{t=1}^{T}x_+^{\mathrm{gr}}(t)}{\sum_{t=1}^{T}x^{\mathrm{hp}}(t)+\sum_{n=1}^{N}x_n^{\mathrm{el}}(t)+b(t)}.$$

B. Simulation Results

The MIQP problem (37)-(39) is solved in the Matlab R2019a environment using Gurobi [21]. The RMPC is tested on three scenarios defined as follows:

- Scenario A: the system includes CELs and NCELs, TLs, PV panel, CHP, HP, auxiliary boiler, TESS, and EESS;
- Scenario B: same as Scenario A without the PV panel;
- Scenario C: same as Scenario A without the HP.

In all the defined scenarios, we assign a weight $\pi=1$ to the penalty cost c^{pen}, so as to encourage self-consumption in the microgrid. The RMPC technique is applied to the system over the whole year 2018 and tested under various robustness conditions. In particular, we vary the robustness factors as follows: $\gamma=\gamma_b=\gamma_q=\gamma_r\in\{0,0.25,0.5,0.75,1\}$, i.e., from no robustness to maximum conservativeness. In Table II we

show for each scenario the values of the performance indices obtained under the various robustness conditions.

The results in Table II show that the minimum EC value is reached in Scenario A, i.e., when all the energy and thermal devices are included in the microgrid, whereas higher costs are incurred in Scenario B and Scenario C, due to the absence of PV generation and HP respectively. It can also be observed that in each test case the EC index increases with the increase of the robustness level, attesting a minimum variation of almost 50% in Scenario A and a maximum variation of almost 70% both in scenarios B and C. As for the SS index, it grows with the robustness level both in Scenarios A and C, while it stays constant and equal to 1 in Scenario B due to the absence of PV generation, as then all the produced energy is locally consumed. In addition, the FESR index decreases with the increase of the robustness level both in Scenarios A and B, while it stays constant and equal to 1 in Scenario C due to the absence of the HP. Finally, the EI index decreases with the increase of the robustness in Scenarios A and C, while it presents the opposite trend in Scenario B, due to the absence of the PV generation.

With the aim of evaluating the effects of the RMPC with respect to the Det-MPC, we assess the constraint violation rate CVR [%] in a Montecarlo simulation with 1000 runs. Such an index measures the number of times a given solution does not satisfy the inequality constraints in (37)-(39) in reference to several realizations of the uncertainty parameters. In particular, we compute the CVR for the considered values of the robustness factors, i.e., $\gamma \in \{0, 0.25, 0.5, 0.75, 1\}$, where $\gamma = 0$ corresponds to the deterministic case while $\gamma = 1$ corresponds to the robust case. Table III shows that the lower the value of the robustness factor, the higher the violation rate. This confirms the effectiveness of the RMPC approach with respect to the Det-MPC approach in achieving a balanced trade-off between performance objective optimization and constraint violation mitigation.

VI. Conclusions and Future Work

In this work we propose a novel robust model predictive control approach for multi-carrier energy microgrids that include thermal and electrical loads (both non-controllable and controllable), renewable energy sources, energy storage systems, heat pumps, and combined heat and power plants. Our aim is to extend the benefits of robust MPC, that has been largely applied to electrical or thermal microgrids, also to the multi-carrier ones, for which only very few contributions have been proposed. The goal of our control strategy is to minimize the overall economical cost and the energy exchange with the main grid, while guaranteeing thermal comfort. Furthermore, the proposed robust MPC approach can deal with uncertainties in the system model, which can be due to external disturbances on loads, renewable energy generation, and electrical and thermal demand. Simulations done for a residential building in the Netherlands and based on a real dataset show the benefits of the proposed approach, allowing the reduction of the electric and thermal balance violation with respect to the deterministic MPC.

Future work will take into account model flexibility in the thermal load demand, as well as the possibility to represent the sale of thermal energy to the district.

Acknowledgments

The authors wish to thank Mr. F. Laterza and Mr. A. Malerba for the fruitful discussions on the control algorithm.

References

[1] X. Fang, S. Misra, G. Xue, and D. Yang. Smart grid — the new and improved power grid: A survey. *IEEE Commun. Surveys Tuts*, 14(4):944–980, 2012.

[2] A. Hirsch, Y. Parag, and J. Guerrero. Microgrids: A review of technologies, key drivers, and outstanding issues. *Renew. Sust. Energ. Rev.*, 90:402–411, 2018.

[3] R. Carli, M. Dotoli, J. Jantzen, M. Kristensen, and S. Ben Othman. Energy scheduling of a smart microgrid with shared photovoltaic panels and storage: The case of the Ballen marina in Samsø. *Energy*, 198:117188, 2020.

[4] E. F. Camacho and C. B. Alba. *Model Predictive Control*. Advanced Textbooks in Control and Signal Processing. Springer London, 2013.

[5] D. Q. Mayne. Model predictive control: Recent developments and future promise. *Automatica*, 50(12):2967–2986, 2014.

[6] H. Bittel, C. N. Jones, and A. Parisio. Use of Model Predictive Control for Short-Term Operating Reserve Using Commercial Buildings in the United Kingdom Context. In *2018 IEEE Decis. Contr. P.*, pages 7308–7313, 2018.

[7] A. Parisio, E. Rikos, and L. Glielmo. A model predictive control approach to microgrid operation optimization. *IEEE Trans. Control Syst. Technol.*, 22(5):1813–1827, 2014.

[8] F. Verrilli, S. Srinivasan, G. Gambino, M. Canelli, M. Himanka, C. Del Vecchio, M. Sasso, and L. Glielmo. Model predictive control-based optimal operations of district heating system with thermal energy storage and flexible loads. *IEEE Trans. Autom. Sci. Eng.*, 14(2):547–557, 2017.

[9] A. Parisio, E. Rikos, and L. Glielmo. Stochastic model predictive control for economic/environmental operation management of microgrids: An experimental case study. *J. Process Contr.*, 43:24–37, 2016.

[10] F. Liberati, A. Di Giorgio, A. Giuseppi, A. Pietrabissa, E. Habib, and L. Martirano. Joint model predictive control of electric and heating resources in a smart building. *IEEE Trans. Ind Appl.*, 55(6):7015–7027, 2019.

[11] F. Alavi, E. Park Lee, N. van de Wouw, B. De Schutter, and Z. Lukszo. Fuel cell cars in a microgrid for synergies between hydrogen and electricity networks. *Appl. Energ.*, 192:296–304, 2017.

[12] M. Pereira, D. Muñoz de la Peña, and D. Limon. Robust economic model predictive control of a community micro-grid. *Renew. Energ.*, 100:3–17, 2017. Special Issue: Control and Optimization of Renewable Energy Systems.

[13] Y. Zhang, L. Fu, W. Zhu, X. Bao, and C. Liu. Robust model predictive control for optimal energy management of island microgrids with uncertainties. *Energy*, 164:1229–1241, 2018.

[14] M. Zhai, Y. Liu, T. Zhang, and Y. Zhang. Robust model predictive control for energy management of isolated microgrids. In *2017 IEEE In. C. Ind. Eng. Eng. Man.*, pages 2049–2053, 2017.

[15] D. Bertsimas and M. Sim. The price of robustness. *Oper. Res.*, 52(1):35–53, 2004.

[16] D. Bertsimas, D. B. Brown, and C. Caramanis. Theory and applications of robust optimization. *SIAM review*, 53(3):464–501, 2011.

[17] A. L. Soyster. Convex programming with set-inclusive constraints and applications to inexact linear programming. *Oper. Res.*, 21(5):1154–1157, 1973.

[18] Neon Neue Energieökonomik, Technical University of Berlin, ETH Zürich, and DIW Berlin. Open-power-system-data. `https://data.open-power-system-data.org/`.

[19] European Commission SETIS. Emhires dataset solarpower. `https://setis.ec.europa.eu/publications/relevant-reports/emhires-dataset-part-ii-solarpower-generation`.

[20] MEKH & VaasaETT Energie-Control. Energy price index. `https://www.energypriceindex.com/latest-update/`.

[21] Gurobi Optimization, Inc. Gurobi optimizer reference manual. https://www.gurobi.com, 2016.